

Prova II

Descrição: prova para ser feita individualmente em casa, com consulta livre a livros e apontamentos

Data de disponibilização: 16 Junho 2020 – 9hs

Prazo máximo para recebimento: 18 Junho 2020 – 19hs

1. No estudo da representação do potencial de uma distribuição localizada de cargas, seguimos a seção 4.1 do Jackson. Faça em detalhe as contas que levam às expressões para os momentos multipolares  $q_{20}$ ;  $q_{21}$ , equação 4.6 desse livro texto.

2. Uma linha de cargas localizada ao longo do eixo  $z$  tem uma densidade linear de carga  $\tau(z)$  e está confinada no intervalo  $-R \leq z \leq R$ .

a) Mostre que a expressão para a carga total do sistema,  $Q = \int_{-R}^R \tau(z') dz'$ , corresponde à densidade volumétrica de carga

$$\rho(\vec{r}') = \frac{\tau(r' \cos \theta')}{2\pi r'^2} [\delta(\cos \theta' - 1) + \delta(\cos \theta' + 1)]$$

b) Calcule as expressões para os momentos multipolares  $q_{\ell m}$  que corresponde a essa distribuição de cargas.

c) Usando a expressão do potencial em termos dos momentos multipolares, mostre que

$$\phi(\vec{r}) = \frac{1}{4\pi\epsilon_0} \sum_{\ell} \left[ \int_{-R}^R \tau(z') z'^{\ell} dz' \right] \frac{P_{\ell}(\cos \theta)}{r^{\ell+1}}$$

3. Na seção 5.7 do Jackson, é obtida a expressão do torque sobre um dipolo magnético. Partindo da equação 5.70,

$$\vec{\tau} = \int \vec{r} \times [\vec{j}(\vec{r}') \times \vec{B}(0)] dV',$$

chega-se a (equação 5.72)

$$\vec{\tau} = \vec{m} \times \vec{B}(0).$$

Para obter esse resultado, o autor faz analogias com outras integrais já feitas. Sem usar esse argumento, mas explorando as técnicas utilizadas na Aula 18 MAI 2020, refaça detalhadamente todas as passagens para obter a expressão acima para o torque.

4. Uma antena é alimentada por um cabo coaxial no modo  $\lambda/4$ , ou seja, cada um de seus ramos tem comprimento  $a = \lambda/4$ . Nessas condições, a corrente na antena tem

que formar um perfil de onda estacionária, ou seja, se anular em  $|z| = a$  e ser máxima em  $z = 0$ , ou seja,

$$I(z', t') = I_0 \cos\left(\frac{\pi z'}{2a}\right) e^{-i\omega t'}$$

a) Partindo da expressão geral para o potencial vetor,

$$\vec{A}(\vec{r}, t) = \frac{\mu_0}{4\pi} \int \frac{[\vec{J}(\vec{r}', t')]_{ret}}{|\vec{r} - \vec{r}'|} dV'; \quad t_{ret} = t - \frac{|\vec{r} - \vec{r}'|}{c}$$

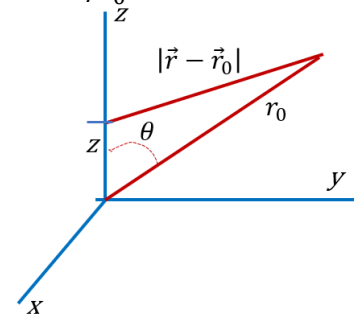
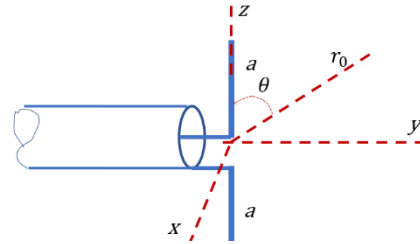
e fazendo o desenvolvimento em série de Taylor apropriado para  $a/r_0 \ll 1$  (veja figura), obtenha a expressão para o potencial vetor

$$\vec{A}(\vec{r}, t) = \frac{\mu_0 I c}{2\pi \omega} \frac{e^{i(kr_0 - \omega t)} \cos\left(\frac{\pi}{2} \cos \theta\right)}{r_0 (\sin \theta)^2} \hat{e}_z$$

b) Escreva a expressão para o potencial vetor em coordenadas esféricas e mostre que o campo magnético é dado por

$$\vec{B}(\vec{r}, t) = i \frac{\mu_0}{2\pi} \frac{\cos\left(\frac{\pi}{2} \sin \theta\right)}{\sin \theta} \frac{I_0 e^{i(kr_0 - \omega t)}}{r_0} \hat{e}_\phi$$

c) Obtenha a expressão para o vetor de Poynting médio  $\langle \vec{S} \rangle$  e esboce a distribuição angular da potência radiada.



5. Num meio ionizado e magnetizado, a relação de dispersão para ondas se propagando ao longo do campo magnético ambiente  $\vec{B}$  tem dois ramos

$$k_D = \frac{\omega}{c} \left[ 1 - \frac{\omega_p^2}{\omega(\omega - \omega_c)} \right]^{1/2}; \quad k_E = \frac{\omega}{c} \left[ 1 - \frac{\omega_p^2}{\omega(\omega + \omega_c)} \right]^{1/2}$$

onde  $\omega_p$  é a frequência de plasma do meio e  $\omega_c$  é a frequência ciclotrônica dos elétrons. A solução  $k = k_D$  corresponde a ondas circularmente polarizadas à direita e a  $k = k_E$  a ondas circularmente polarizadas à esquerda.

a) Considere  $\omega_p > \omega_c$  e faça um diagrama de dispersão (gráfico  $\omega \times k$ ), mostrando esquematicamente os dois ramos da relação de dispersão. Em particular, indique claramente no gráfico

- frequências de corte dos dois ramos ( $k \rightarrow 0$ )
- comportamento assintótico dos dois ramos quando ( $\omega \rightarrow \infty$ )
- quais modos se propagam na condição  $\omega \ll \omega_c$
- regiões em que nenhum dos modos se propagam

b) Considerando ainda a condição  $\omega \ll \omega_c$ , determine as expressões para as velocidades de fase,  $v_f$ , e de grupo,  $v_g$ .

6. Neste problema, vamos obter a expressão para o campo eletromagnético produzido por um plano de cargas que oscilam periodicamente com o tempo. Considere uma distribuição superficial uniforme de cargas no plano  $(x, y)$ , de forma que a densidade de cargas seja dada por

$$\rho(\vec{r}, t) = \sigma\delta(z); \quad \sigma \text{ constante}$$

Suponha que as cargas oscilem periodicamente em torno de sua posição de equilíbrio com velocidade

$$\vec{v}(t) = v_0 \cos(\omega t) \hat{e}_x$$

Como a densidade de cargas é constante, o potencial escalar também é constante, de forma que o campo eletromagnético resultante será associado somente ao potencial vetor produzido pela densidade de corrente

$$\vec{j}(\vec{r}, t) = \sigma v_0 \delta(z) \cos(\omega t) \hat{e}_x$$

a) Usando a técnica de escrever

$$[\vec{G}(\vec{r}', t')]_{ret} = \int \vec{G}(\vec{r}', t') \delta(t' - t_{ret}) dt'$$

empregada no problema 4 da Série de Exercícios 6, mostre que o potencial vetor pode ser escrito como

$$\vec{A}(\vec{r}, t) = \frac{\mu_0}{4\pi} \sigma v_0 \hat{e}_x \int \Gamma(\vec{r}, t - t') \cos(\omega t') dt'$$

onde

$$\Gamma(\vec{r}, t - t') = \int \frac{\delta \left[ t - t' - \frac{1}{c} \sqrt{(x - x')^2 + (y - y')^2 + z^2} \right]}{\sqrt{(x - x')^2 + (y - y')^2 + z^2}} dx' dy'$$

b) Para fazer a integral para  $\Gamma(\vec{r}, t - t')$ , utilize coordenadas polares, isto é,

$$x' - x = \ell \cos \theta; \quad y' - y = \ell \sin \theta; \quad dx' dy' = \ell d\ell d\theta$$

e simplifique o argumento da função delta definindo a variável

$$s = \frac{1}{c} \sqrt{\ell^2 + z^2} - \Delta t; \quad \Delta t = t - t'$$

Obtenha, então,

$$\Gamma(\vec{r}, t - t') = 2\pi c \int_{\frac{|z|}{c} - \Delta t}^{\infty} \delta(s) ds = 2\pi c \Theta \left( t - t' - \frac{|z|}{c} \right)$$

onde  $\Theta(s)$  é a função degrau.

c) Utilizando esse resultado, obtenha a expressão para o potencial vetor

$$\vec{A}(\vec{r}, t) = \frac{\mu_0}{2} \sigma v_0 c \hat{e}_x \int_{-\infty}^{t - \frac{|z|}{c}} \cos(\omega t') dt' = \frac{E_0}{\omega} \sin\left(t - \frac{|z|}{c}\right) \hat{e}_x; \quad E_0 = \frac{1}{2} \mu_0 \sigma v_0 c$$

(Nesse resultado, o valor constante do potencial vetor no infinito foi igualado a zero, já que não afeta as expressões para os campos).

c) Determine a expressão do vetor de Poynting deste campo, para  $z > 0$ .

7. Uma técnica muito empregada em laboratórios de esfriamento a laser para aprisionamento de átomos é fazer o feixe atômico se propagar ao longo do eixo de um solenoide que produz um campo magnético axial da forma

$$B(z) = B_b + B_o \sqrt{1 - \beta z}$$

onde  $B_b$ ,  $B_o$  e  $\beta$  são constantes. Este campo causa um efeito Zeeman que varia com a posição, compensando o deslocamento Doppler dos átomos em movimento, os mantendo em ressonância com o laser enquanto desaceleram. Como o feixe atômico tem certa abertura, é importante conhecer o campo magnético fora do eixo para determinar como o laser interage com os átomos dentro do solenoide.

O cálculo dessas componentes pode ser feito analiticamente utilizando uma técnica descrita no trabalho de pesquisadores do Instituto de Física de São Carlos,

S.R. Muniz, V.S. Bagnato e M. Bhattacharya; *Am. J. Phys.* **83**, 513 (2015).

Estude o método por eles desenvolvido, nas três primeiras seções do artigo, e depois faça todas as passagens que levam as expressões do potencial e das componentes do campo na seção 4 do artigo, especificamente, equações (18), (19), (20), (21) e (22).

OBS: O artigo referenciado está em anexo.

# Analysis of off-axis solenoid fields using the magnetic scalar potential: An application to a Zeeman-slower for cold atoms

Sérgio R. Muniz, Vanderlei S. Bagnato, and M. Bhattacharya

Citation: *American Journal of Physics* **83**, 513 (2015); doi: 10.1119/1.4906516

View online: <https://doi.org/10.1119/1.4906516>

View Table of Contents: <https://aapt.scitation.org/toc/ajp/83/6>

Published by the [American Association of Physics Teachers](#)

---

## ARTICLES YOU MAY BE INTERESTED IN

### [Magnetic field of a cylindrical coil](#)

*American Journal of Physics* **74**, 621 (2006); <https://doi.org/10.1119/1.2198885>

### [Cylindrical magnets and ideal solenoids](#)

*American Journal of Physics* **78**, 229 (2010); <https://doi.org/10.1119/1.3256157>

### [Magnetic field of a finite solenoid with a linear permeable core](#)

*American Journal of Physics* **79**, 1030 (2011); <https://doi.org/10.1119/1.3602096>

### [Magnetic field due to a solenoid](#)

*American Journal of Physics* **52**, 258 (1984); <https://doi.org/10.1119/1.13936>

### [Electromagnetic mirrors in the sky: Accessible applications of Maxwell's equations](#)

*American Journal of Physics* **83**, 506 (2015); <https://doi.org/10.1119/1.4913412>

### [The Magnetic Scalar Potential](#)

*American Journal of Physics* **39**, 1357 (1971); <https://doi.org/10.1119/1.1976655>

---



# Analysis of off-axis solenoid fields using the magnetic scalar potential: An application to a Zeeman-slower for cold atoms

Sérgio R. Muniz and Vanderlei S. Bagnato

*Instituto de Física de São Carlos, Universidade de São Paulo, São Carlos, SP 13560-970, Brazil*

M. Bhattacharya

*School of Physics and Astronomy, Rochester Institute of Technology, 84 Lomb Memorial Drive, Rochester, New York 14623*

(Received 15 March 2010; accepted 13 January 2015)

In a region free of currents, magnetostatics can be described by the Laplace equation of a scalar magnetic potential, and one can apply the same methods commonly used in electrostatics. Here, we show how to calculate the general vector field inside a real (finite) solenoid, using only the magnitude of the field along the symmetry axis. Our method does not require integration or knowledge of the current distribution and is presented through practical examples, including a nonuniform finite solenoid used to produce cold atomic beams via laser cooling. These examples allow educators to discuss the nontrivial calculation of fields off-axis using concepts familiar to most students, while offering the opportunity to introduce themes of current modern research. © 2015 American Association of Physics Teachers.

[<http://dx.doi.org/10.1119/1.4906516>]

## I. INTRODUCTION

Magnetic fields produced by solenoids and axially symmetric coils are ubiquitous, and the ability to calculate them is an integral part of training in physics. Time constraints, however, tend to focus the attention of most introductory electromagnetism (EM) courses on the analytical solution of only a few highly symmetrical cases, such as the field along the axis of a circular coil or inside an infinite solenoid.<sup>1–5</sup> Nevertheless, many applications require at least an estimate of the full vector field in regions away from the axis,<sup>6–8</sup> which involve mathematical tools often not discussed at the introductory level. On the other hand, most EM courses already dedicate a fair amount of time teaching students to identify and solve electrostatic problems using the Laplace equation. In some cases, the same methods can be applied to magnetostatic problems, sometimes leading to useful insights.

Sadly, most students do not appreciate the similarities between the two classes of problems<sup>9</sup> due to a limited exposure to practical examples involving the magnetic potential. We feel that the ability to make use of the magnetic potential is useful,<sup>10,11</sup> particularly because scalar potentials are generally more intuitive and easier to visualize. Besides, a unified treatment could be pedagogically relevant in generalizing the discussion of the multipole expansions.<sup>12–14</sup> Therefore, the primary goal here is to present a couple of pedagogical examples illustrating the application of the magnetic potential method to real solenoids.

In addition, these examples also offer the opportunity to discuss in the classroom axisymmetric fields evaluated off-axis, without the need to introduce the formalism of elliptic integrals. Although other methods for finding off-axis magnetic fields have been mentioned earlier in the literature,<sup>6,7</sup> to our knowledge, it has not been presented from such a simple and intuitive viewpoint.

As further motivation, we have chosen an example that brings a real and practical application from the cutting edge of research into the classroom: a nonuniform solenoid used in many research laboratories to produce beams of slow (cold) atoms. This solenoid, known as a Zeeman-slower,<sup>15–17</sup> is used in conjunction with appropriately prepared laser beams to

slow down and cool neutral atoms, from hundreds of Kelvin to milliKelvin temperatures, by combining the action of radiation pressure with the Zeeman effect. This device is one of the key developments in the area of laser cooling,<sup>18,19</sup> and one of the enabling technologies leading to the 1997 Nobel prize in Physics.<sup>20</sup> The techniques for laser cooling and trapping of atoms have produced many dramatic advancements in our understanding of quantum physics,<sup>21</sup> including the achievement of Bose-Einstein condensation, which was recognized with another Nobel prize<sup>20</sup> in 2001. In both cases, magnetic fields were an important part of experimental design and data interpretation. Educators can use the solenoid discussed here, as well as the references herein, to introduce and discuss some of these modern developments in quantum physics, making the subject more interesting to students.

## II. REVIEWING SOME BASIC CONCEPTS

We begin here by recalling the fundamental equation of magnetostatics:  $\vec{\nabla} \times \vec{H} = \vec{J}$ , where  $\vec{H}$  is the magnetic field and  $\vec{J}$  the current density. Typically,  $\vec{H}$  is related to the magnetic induction field  $\vec{B}$  by some constitutive relation expressing the properties of a particular material. For linear and isotropic materials with magnetic permeability  $\mu$ ,  $\vec{B} = \mu\vec{H}$  and in a current-free region  $\vec{\nabla} \times \vec{B} = 0$ , implying that  $\vec{B} = -\vec{\nabla}\phi_M$ . Since Maxwell's equations also state that  $\vec{\nabla} \cdot \vec{B} = 0$ , this results in  $\nabla^2\phi_M = 0$ , which is Laplace's equation for the magnetic (scalar) potential  $\phi_M$ , in any current-free region.

Although Laplace's equation is only typically valid in a region free of charges or currents, they are allowed to exist on or outside a surface  $S$  surrounding that region. The solutions of Laplace's equation present three important properties: superposition, smoothness, and uniqueness. The property of superposition results from the fact that Laplace's equation is a linear equation. Smoothness implies that no solution in a region  $V$  of space, bounded by a surface  $S$ , can present either a maximum or a minimum within  $V$  (extreme values can occur only at the surface  $S$ ). The third property is the one most relevant to us here; it states<sup>3</sup> that if one finds a solution  $\phi_M$  in a region of space consistent with the

prescribed boundary conditions, then that solution is unique up to an additive constant. Therefore, it does not matter which particular method is used to find the solution. Once an appropriate solution is found, we know it is the *only* solution.

Despite the obvious similarities between the electrostatic and magnetic potentials, there are indeed reasons why the analogy can only be taken so far<sup>9,12</sup> and why it is not widely explored further in textbooks. The first one arises whenever  $\vec{J} \neq 0$ , in which case it is not trivial to write a relation between  $\phi_M$  and  $\vec{J}$ . The second complication occurs due to the fact that the scalar potential is generally a multiply valued function, requiring a prescription specifying where it can be used. However, as shown by Bronzan,<sup>12</sup> these complications can be overcome, permitting one to exploit the advantages of a magnetic scalar potential.

### III. THE MAGNETIC FIELD OF A FINITE UNIFORM SOLENOID

Let us start by considering axisymmetric fields produced by a solenoid (see Fig. 1). Because of the axisymmetric symmetry of this problem, the field on the  $z$ -axis can only depend on  $z = r \cos \theta$  and must point in the  $\pm z$ -direction. The magnetic potential can be found using as boundary condition the magnitude of the field along the  $z$ -axis,  $B_z(z)$ , which is readily available through simple summation formulas over the approximately circular coils forming the solenoid or by direct measurement along the axis.

For generality and convenience, we describe the problem using spherical coordinates, where the solution of the axisymmetric scalar potential  $\phi_M$  can be written in the form

$$\phi_M(r, \theta) = \sum_{\ell=0}^{\infty} \left( a_{\ell} r^{\ell} + \frac{b_{\ell}}{r^{\ell+1}} \right) P_{\ell}(\cos \theta), \quad (1)$$

where  $a_{\ell}$  and  $b_{\ell}$  are the coefficients to be determined, and  $P_{\ell}$  represents a Legendre polynomial of order  $\ell$ . Because we are mainly interested in the values of the field inside the solenoid, we set  $b_{\ell} = 0$  to avoid a singularity at  $r = 0$ . As a result, the potential takes the simpler form

$$\phi_M(r, \theta) = a_0 + a_1 r P_1(\cos \theta) + a_2 r^2 P_2(\cos \theta) + \dots, \quad (2)$$

---


$$\phi_M(r, \theta) = -\frac{\alpha L r \cos \theta}{(R^2 + L^2/4)^{1/2}} + \frac{3}{2} \left( \frac{5}{3} \cos^3 \theta - \cos \theta \right) \times \left[ \frac{L \alpha}{2(R^2 + L^2/4)^{3/2}} - \frac{L^3 \alpha}{8(R^2 + L^2/4)^{5/2}} \right] r^3 + \dots \quad (9)$$

Finally, using this potential one can calculate the components  $B_r$  and  $B_{\theta}$  of the magnetic field as

$$B_r = -\frac{\partial \phi_M(r, \theta)}{\partial r} = \frac{\alpha L \cos \theta}{(R^2 + L^2/4)^{1/2}} - \frac{3}{2} (5 \cos^3 \theta - 3 \cos \theta) \times \left[ \frac{L \alpha}{2(R^2 + L^2/4)^{3/2}} - \frac{L^3 \alpha}{8(R^2 + L^2/4)^{5/2}} \right] r^2 + \dots, \quad (10)$$

and

$$B_{\theta} = -\frac{1}{r} \frac{\partial \phi_M(r, \theta)}{\partial \theta} = -\frac{L \alpha \sin \theta}{(R^2 + L^2/4)^{1/2}} - \frac{3}{2} (\sin \theta - 5 \cos^2 \theta \sin \theta) \times \left[ \frac{L \alpha}{2(R^2 + L^2/4)^{3/2}} - \frac{L^3 \alpha}{8(R^2 + L^2/4)^{5/2}} \right] r^2 + \dots \quad (11)$$

and for points along the  $z$ -axis becomes

$$\phi_M(z) = a_0 + a_1 z + a_2 z^2 + a_3 z^3 + \dots \quad (3)$$

Equation (3) is a Taylor series about the point  $z = 0$ , so the coefficients are given by

$$a_{\ell} = \frac{1}{\ell!} \left( \frac{\partial^{\ell} \phi_M}{\partial z^{\ell}} \right)_{z=0}. \quad (4)$$

In this way, the full scalar potential in Eq. (2) becomes analytically determinable, allowing us to evaluate  $\vec{B} = -\vec{\nabla} \phi_M$  at any point in space.

As a first example, let us consider the case of a finite solenoid of length  $L$  and radius  $R$  carrying a uniform current  $I$ , as illustrated in Fig. 1. If the solenoid has  $N$  turns per unit length, the magnetic field along the  $z$ -axis can be calculated by integrating the expression for the axial field of a circular current loop,<sup>1</sup> giving

$$B(z) = \alpha \left( \frac{z_+}{\sqrt{R^2 + z_+^2}} - \frac{z_-}{\sqrt{R^2 + z_-^2}} \right), \quad (5)$$

where  $z_{\pm} = z \pm L/2$  and  $\alpha = \mu_0 N I / 4\pi$  in SI units. Now, since

$$B_z(z) = -\frac{\partial \phi_M}{\partial z}, \quad (6)$$

we can write

$$\phi_M(z) = -\int B(z') dz'. \quad (7)$$

Using Eq. (5) in Eq. (7), we obtain the general form of the potential for the finite solenoid along the axis:

$$\phi_M(z) = -\alpha \left( \sqrt{R^2 + z_+^2} - \sqrt{R^2 + z_-^2} \right). \quad (8)$$

Expanding Eq. (8) in a Taylor series about  $z = 0$ , we get the various coefficients for  $\phi_M(z)$ . Then, using these coefficients in Eq. (2), we find the scalar potential valid everywhere inside the solenoid as

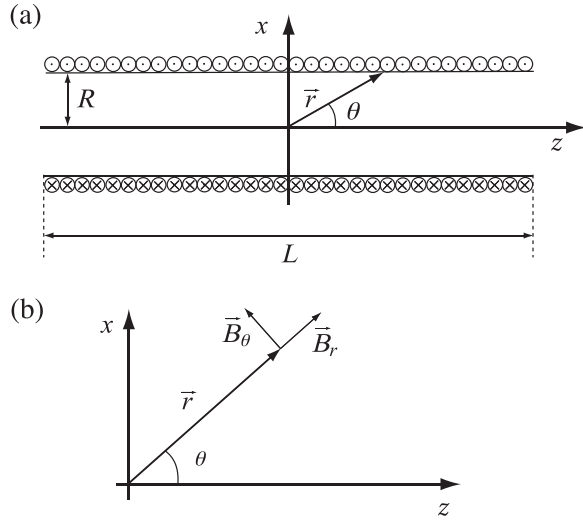


Fig. 1. (a) Schematic representation of a finite and homogenous solenoid. The crosses (dots) represent current flowing into (out of) the page. (b) The relevant coordinates and field directions.

We note that these results give (approximate) analytical results for the magnetic field everywhere inside the solenoid, with their precision limited only by the number of terms included in the power series expansion. One can test these results by comparing Eqs. (9) and (10) with those presented in Chapter 5 of Ref. 2, where a different method was used to evaluate the field components. In particular, we will show that if one keeps only the first order term in the expansion, the result simplifies to the approximate solution given in problem 5.2. To begin, we recall the relations

$$B_\rho = B_r \sin \theta + B_\theta \cos \theta, \quad (12)$$

$$B_z = B_r \cos \theta - B_\theta \sin \theta, \quad (13)$$

from which we obtain, up to third order,

$$B_\rho \simeq \frac{3\alpha LR^2 r^2}{2(R^2 + L^2/4)^{5/2}} \sin \theta \cos \theta. \quad (14)$$

Finally, using  $\rho = r \sin \theta$  and  $z = r \cos \theta$  in the limit  $R \ll L$ , we find

$$B_\rho(\rho, z) \simeq \frac{96\pi NI}{c} \left( \frac{R^2 z \rho}{L^4} \right), \quad (15)$$

which is expressed here in CGS units (with  $\alpha = 2\pi NI/c$ ) to facilitate direct comparison with Ref. 2.

In Fig. 2, we compare the results obtained by keeping the first eight terms in the series expansion (solid curve), corresponding to the 15th order in  $r$ , against numerical simulations of the field (dots/circles) using a direct summation over the exact analytical expression (elliptic integrals) for each individual coil of the finite solenoid. In addition, Fig. 2 also shows the good partial agreement obtained using the third-order approximation (dashed curve), extending to distances up to about half the size of the solenoid. Note that, for a real finite system, the disagreement increases rapidly after some point (for  $|z| \geq 0.25$  for third order and  $|z| \geq 0.5$  for 15th order). The agreement can be improved significantly by

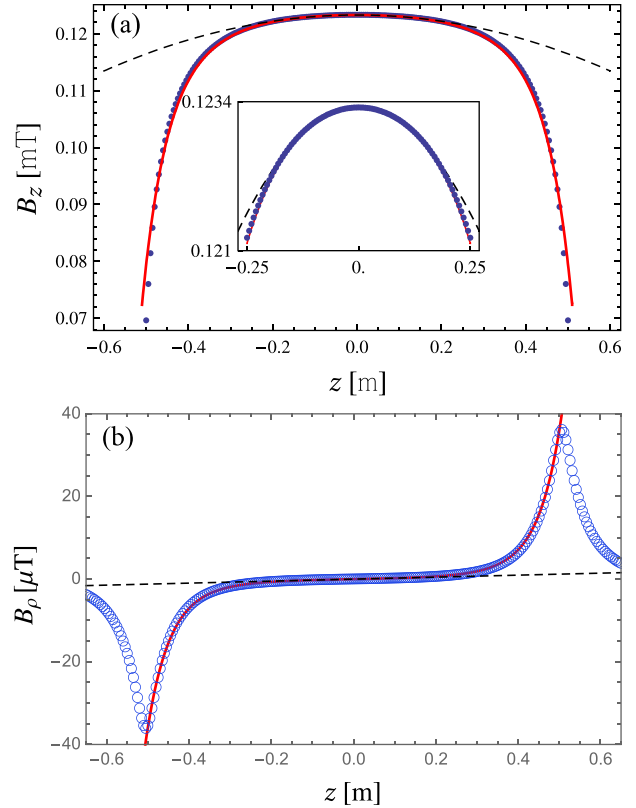


Fig. 2. Comparison of the power series approximation (solid and dashed curves) with a numerical simulation (points/circles) of the exact field (using elliptic integrals) for a uniform solenoid ( $L = 1$  m,  $R = 10$  cm, and  $N = 100$ ) carrying a current of  $I = 1$  A. We plot both the axial field (a) and the transverse field (b) profiles. All results are evaluated off-axis ( $\rho = 8$  cm) and the power series results are shown for expansions up to third (dashed) and 15th (solid) orders. The inset in (a) shows the good agreement obtained near  $z = 0$ , even for the third-order approximation.

including higher-order terms, allowing for a much better approximation near the edges, as shown in Fig. 2. However, due to the simplifications made, the power series approximation still does not contain all the physics of the problem. For instance, it does not accurately describe the field outside the solenoid. Nevertheless, the magnetic potential method presented here still provides a reasonable representation of the internal fields up to the very end of the solenoid.

#### IV. THE ZEEMAN-SLOWER: AN INHOMOGENEOUS FINITE SOLENOID

We now consider a practical problem, familiar to many atomic physics laboratories, which is the design of a solenoid capable of producing a field on the  $z$ -axis of the form

$$B(z) = B_b + B_0 \sqrt{1 - \beta z}, \quad (16)$$

where  $B_b$ ,  $B_0$ , and  $\beta$  are constants. Such a field is suitable for slowing atomic beams using laser light.<sup>15</sup> The field of Eq. (16) causes a spatially varying Zeeman effect that compensates for the changing Doppler shift of the moving atoms, thus keeping them in resonance with the light as they decelerate along the beam path. This technique is called Zeeman slowing,<sup>15</sup> and the shape is chosen to keep the radiation pressure constant, typically with a particle acceleration of  $\sim 10^6$  m/s<sup>2</sup> throughout the Zeeman solenoid<sup>17</sup> (see Fig. 3).

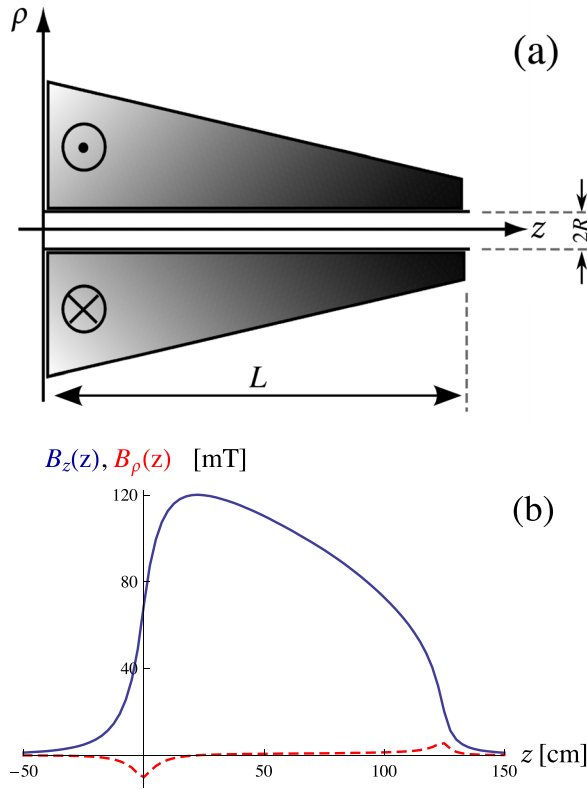


Fig. 3. (a) Sketch of a tapered (triangular shape) solenoid creating an inhomogeneous current distribution to produce the appropriate axial field profile (b) for a Zeeman solenoid, with  $L = 125$  cm,  $R = 4$  cm, and  $B_{\max} \approx 120$  mT. The solid line shows  $B$  ( $= B_z$ ) along the axis ( $\rho = 0$ ), whereas the dashed line represents the transverse field  $B_\rho$  at  $\rho = 2.5$  cm.

In general, the atomic beam encompasses a certain solid angle as it traverses the solenoid and most atoms follow trajectories that do not lie exactly on the axis. Since the resonance condition with the laser depends on both the magnitude (via detuning) and direction (via polarization) of the magnetic field, the knowledge of the off-axis field is important in understanding how light interacts with atoms at different points inside the solenoid.

In this case, the magnetic potential along the  $z$ -axis takes the form

$$\phi_M(z) = - \int B(z') dz' = -B_b z + \frac{2B_0}{3\beta} (1 - \beta z)^{3/2}, \quad (17)$$

where the constant of integration has been suppressed. Following the same steps as in Sec. III and after calculating the derivatives and solving for the coefficients  $a_\ell$ , we obtain the general form of the magnetic potential for the Zeeman solenoid:

$$\begin{aligned} \phi_M(r, \theta) = & \frac{2B_0}{3\beta} - (B_b + B_0)r \cos \theta \\ & + \frac{B_0}{\sqrt{\pi}} \sum_{n=2}^{\infty} \frac{\beta^{n-1} \Gamma\left(n - \frac{1}{2}\right)}{n!(2n-3)} r^n P_n(\cos \theta), \end{aligned} \quad (18)$$

where  $\Gamma(n)$  is the gamma function. Calculating the spherical components of the magnetic field then gives

$$\begin{aligned} B_r(r, \theta) = & (B_b + B_0) \cos \theta \\ & - \frac{B_0}{\sqrt{\pi}} \sum_{n=2}^{\infty} \frac{\beta^{n-1} \Gamma\left(n - \frac{1}{2}\right)}{(n-1)!(2n-3)} r^{n-1} P_n(\cos \theta) \end{aligned} \quad (19)$$

and

$$\begin{aligned} B_\theta(r, \theta) = & -(B_b + B_0) \sin \theta \\ & - \frac{B_0}{\sqrt{\pi} \sin \theta} \sum_{n=2}^{\infty} \frac{\beta^{n-1} \Gamma\left(n - \frac{1}{2}\right)}{(n-1)!(2n-3)} r^{n-1} \\ & \times [\cos \theta P_n(\cos \theta) - P_{n-1}(\cos \theta)]. \end{aligned} \quad (20)$$

The transverse and axial components can be obtained from Eq. (13), giving

$$\begin{aligned} B_\rho(\rho, z) = & \frac{-B_0}{\sqrt{\pi}} \sum_{n=2}^{\infty} \frac{\beta^{n-1} \Gamma\left(n - \frac{1}{2}\right)}{(n-1)!(2n-3)} \\ & \times \frac{(\sqrt{z^2 + \rho^2})^n}{\rho} [P_n(\tilde{z}) - \tilde{z} P_{n-1}(\tilde{z})] \end{aligned} \quad (21)$$

and

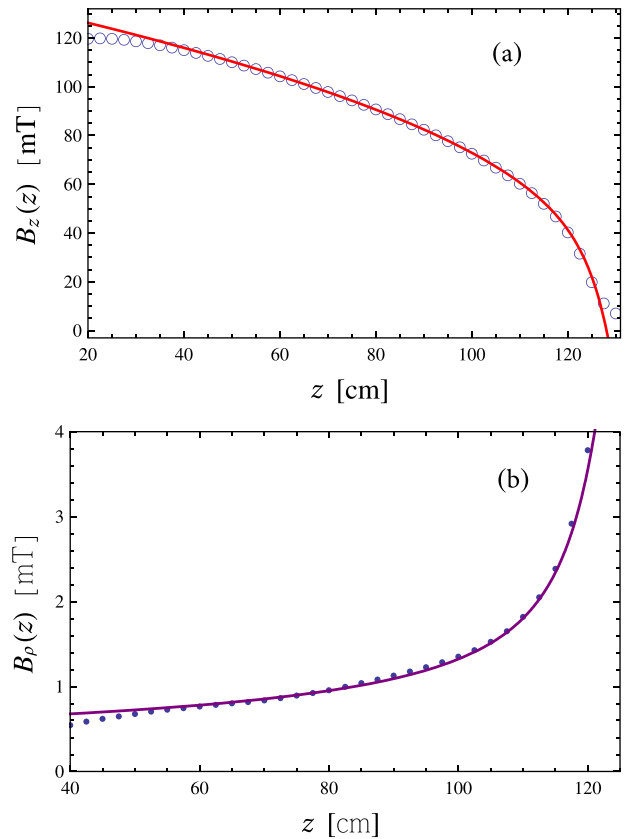


Fig. 4. Comparison for the series solutions of the Zeeman solenoid for  $B_z$  with  $\rho = 0$ , and  $B_\rho$  with  $\rho = 2.5$  cm. The points represent the actual experimental field and the solid lines are the analytical (series) approximations [Eqs. (21) and (22)] of the model function in Eq. (16).

$$B_z(\rho, z) = (B_b + B_0) - \frac{B_0}{\sqrt{\pi}} \sum_{n=2}^{\infty} \frac{\beta^{n-1} \Gamma\left(n - \frac{1}{2}\right)}{(n-1)!(2n-3)} \times \left(\sqrt{z^2 + \rho^2}\right)^{n-1} P_{n-1}(\tilde{z}), \quad (22)$$

where we have introduced the shorthand  $\tilde{z} = z/\sqrt{z^2 + \rho^2}$ .

Notice that the transverse component of the magnetic field inside the Zeeman-slower does not depend on  $B_b$ . Also, note that  $B_\rho = 0$  at  $\rho = 0$  (on-axis), as expected, and it can be verified that the on-axis field sums back to the exact expression of Eq. (16). Although caution may be necessary when evaluating the field for  $\rho = 0$  ( $\theta = 0$ ), the careful use of L'Hospital's rule ensures finite and correct answers.

Now, to compare these analytical approximations (series solutions) to the actual field, shown in Fig. 4, we will use a different approach. The motivation is to mimic a situation where the current distribution that generates the field may not be known exactly, but the axial field can be measured directly in the laboratory. This could be the case in a real application, where imperfections in the winding pattern often are not considered in the ideal model. From the experimental data, one can then build a mathematical model by using either a fitting function (if the functional form is known or can be easily guessed) or by using an interpolating function, such as a polynomial, to represent the data in a limited region of space. Here, since the approximate functional form of the axial field is known, we will extract the model parameters by numerically fitting the data in Fig. 4, to  $B_z(z)$  in Eq. (16), and substituting them into Eqs. (21) and (22). Note that the limitations of this type of modeling may result in some inaccuracies, particularly close to the edges, where fringe effects are important. In any practical situation, one may need to explore different approaches to find a mathematical model that is accurate enough in the region of interest.

After following these steps to model the data, we show in Fig. 4 a comparison between the series solution and the real field. There is a reasonable agreement between the solid lines, representing Eq. (21) and Eq. (22), and the data points. Note that, in contrast to the uniform finite solenoid where a power series was used to approximate the exact solution, here the power series simply approximates our model<sup>22</sup> (fitting) function. Therefore, increasing the order<sup>23</sup> of the series expansion only improves the agreement with the model function, which represents the data only over a limited region and does not contain all the information in the problem. This is clearly visible in Fig. 4, where good agreement is found only in the range  $z \approx 0.4\text{--}1.2\text{ m}$ .

## V. CONCLUSION

Using the simple concept of the magnetostatic scalar potential, and only the knowledge of the field along the symmetry axis, we have shown how to determine the magnetic field anywhere inside an inhomogeneous finite solenoid, without explicitly integrating (or even knowing) the current distribution. In cases where the current distribution is known, but the expression for the off-axis field is nontrivial (for instance, given by elliptical integrals), one can still gain some insight by using the method described here. This simple analysis follows from a straightforward analogy with the electrostatic boundary value problem and can be useful in determining

field inhomogeneities in various practical experiments involving solenoids. In the present article, we have used an example from contemporary experiments in atomic physics to demonstrate the method. However, we believe that a simplified version of this discussion (e.g., the uniform finite solenoid) could be used in an undergraduate classroom as a practical example of a calculation of off-axis magnetic fields.

## ACKNOWLEDGMENTS

The authors acknowledge Kevin M. Jones, from Williams College, Kris Helmersen, from Monash University, and Kevin C. Wright, from Dartmouth College, for their critical reading of the manuscript and suggestions.

- <sup>1</sup>D. J. Griffiths, *Introduction to Electrodynamics*, 3rd ed. (Prentice-Hall, Upper Saddle River, NJ, 1999).
- <sup>2</sup>J. D. Jackson, *Classical Electrodynamics*, 2nd ed. (J. Wiley, New York, 1974), Chaps. 1, 3 and 5 (and particularly Problem 5.2).
- <sup>3</sup>M. A. Heald and J. B. Marion, *Classical Electromagnetic Radiation*, 3rd ed., Chap. 3 has a good discussion of the Laplace equation (Saunders/Harcourt Brace, Fort Worth, TX, 1994).
- <sup>4</sup>B. B. Dasgupta, "Magnetic field due to a solenoid," *Am. J. Phys.* **52**, 258 (1984).
- <sup>5</sup>V. Labinac, N. Erceg, and D. Kotnik-Karuza, "Magnetic field of a cylindrical coil," *Am. J. Phys.* **74**, 621–627 (2006).
- <sup>6</sup>R. H. Jackson, "Off-axis expansion solution of Laplace's equation: Application to accurate and rapid calculation of coil magnetic fields," *IEEE Trans. Electron Devices* **46**, 1050–1062 (1999).
- <sup>7</sup>J. T. Conway, "Exact solutions for the magnetic fields of axisymmetric solenoids and current distributions," *IEEE Trans. Magn.* **37**, 2977–2988 (2001).
- <sup>8</sup>M. I. Grivich and D. P. Jackson, "The magnetic field of current-carrying polygons: An application of vector field rotations," *Am. J. Phys.* **68**, 469–474 (2000).
- <sup>9</sup>M. J. Lahart, "Use of electromagnetic scalar potentials in boundary value problems," *Am. J. Phys.* **72**, 83–91 (2004).
- <sup>10</sup>B. B. Dasgupta, "A novel method of solving electrostatic potential problems," *Am. J. Phys.* **53**, 971–973 (1985).
- <sup>11</sup>B. Irvine, M. Kemnetz, A. Gangopadhyaya, and T. Ruubel, "Magnet traveling through a conducting pipe: A variation on the analytical approach," *Am. J. Phys.* **82**, 273–279 (2014).
- <sup>12</sup>J. B. Bronzan, "The magnetic scalar potential," *Am. J. Phys.* **39**, 1357–1359 (1971).
- <sup>13</sup>C. G. Gray, "Simplified derivation of the magnetostatic multipole expansion using the scalar potential," *Am. J. Phys.* **46**, 582–583 (1978).
- <sup>14</sup>C. G. Gray, "Magnetic multipole expansion using the scalar potential," *Am. J. Phys.* **47**, 457–459 (1979).
- <sup>15</sup>W. D. Phillips and H. Metcalf, "Laser deceleration of an atomic beam," *Phys. Rev. Lett.* **48**, 596–599 (1982); W. D. Phillips and H. J. Metcalf, "Cooling and trapping atoms," *Sci. Am.* **256**, 50–56 (1987).
- <sup>16</sup>C. J. Dedman, J. Nes, T. M. Hanna, R. G. Dall, K. G. H. Baldwin, and A. G. Truscott, "Optimum design and construction of a Zeeman slower for use with a magneto-optic trap," *Rev. Sci. Instrum.* **75**, 5136–5142 (2004).
- <sup>17</sup>H. J. Metcalf and P. van der Straten, *Laser Cooling and Trapping* (Springer-Verlag, New York, 1999).
- <sup>18</sup>See open article at <http://focus.aps.org/story/v21/st11>; W. D. Phillips, P. L. Gould, and P. D. Lett, "Cooling, stopping and trapping atoms," *Science* **239**, 877–883 (1988); S. Chu, "Laser trapping of neutral particles," *Sci. Am.* **266**, 70–76 (1992).
- <sup>19</sup>S. C. Zilio and V. S. Bagnato, "Radiative forces on neutral atoms—A classical treatment," *Am. J. Phys.* **57**, 471–474 (1989).
- <sup>20</sup>For more information visit the official Nobel prize website at <[http://www.nobelprize.org/nobel\\_prizes/physics](http://www.nobelprize.org/nobel_prizes/physics)>.
- <sup>21</sup>See review articles on special *Nature Insight* issue on Ultracold Matter. K. Southwell, *Nature* **416**, 205–246 (2002).
- <sup>22</sup>The fitting yields  $B_b = 27.6\text{ mT}$ ,  $B_0 = 132.8\text{ mT}$ , and  $\beta = 0.544\text{ m}^{-1}$ .
- <sup>23</sup>For the agreement shown in Fig. 4, 70 terms were kept.